Sum-Frequency Vibrational Spectroscopy of CO Adsorption on Pt(111) and Pt(110) Electrode Surfaces in Perchloric Acid Solution: Effects of Thin-Layer Electrolytes in Spectroelectrochemistry

F. Dederichs,[†,§] K. A. Friedrich,[‡] and W. Daum*[,†]

Institut für Grenzflächenforschung und Vakuumphysik, Forschungszentrum Jülich, D-52425 Jülich, Germany, and Physik Department E19, Technische Universität München, D-85748 Garching, Germany

Received: March 9, 2000; In Final Form: May 4, 2000

We present and discuss sum-frequency vibrational spectra of CO adsorbed on (111)- and (110)-oriented Pt single-crystal electrodes in a 0.1 M $HClO_4$ aqueous electrolyte. For potentials slightly above the potential of hydrogen evolution, CO adsorbs on terminal and 3-fold hollow sites of the Pt(111) surface with frequencies of 2066 cm^{-1} and 1788 cm^{-1}, respectively. Around 0.4 V versus RHE, a structural transition of the CO adlayer takes place with the spectroscopic signature of terminal and bridge-like coordinations (∼2065 cm^{-1} and 1850 cm^{-1}, respectively). Only terminal adsorption is observed for the (110) surface. Although these frequencies of the CO stretching vibrations are in good agreement with previous infrared reflection−absorption studies, our sum-frequency generation (SFG) spectra indicate a complete oxidation and removal of the CO adlayer at potentials of ∼0.55 V for Pt(111) and ∼0.45 V for Pt(110), well below the respective main oxidation potentials in cyclic voltammetry. We show that the lower oxidation potentials observed in SFG are specific for a CO-depleted thin-layer electrolyte and that the CO depletion results from the combination of CO oxidation in the layer and limited diffusion of CO from the bulk electrolyte. We do not find indications for CO adsorbed in a state which is invisible to SFG, as reported in a recent study of CO adsorption on Pt(111) in 0.5 M H_2SO_4 (S. Baldelli et al. *J. Phys. Chem. B* **1999**, *103*, 8920.

I. Introduction

Currently, there is considerable interest in CO adsorption on Pt electrodes, partly motivated by the crucial role of CO adsorption in electrocatalytic reactions[1] but also because CO adlayers on Pt single-crystal electrodes represent well-defined model systems for covalently bound adsorbates. The latter aspect is particularly true for the Pt(111) surface, for which the local adsorption configuration and the long-range structures of CO adlayers have been extensively characterized. Our present knowledge of CO adsorption on metal electrodes is predominantly based upon experimental results obtained by three in situ techniques: cyclic voltammetry (CV), infrared reflection−absorption spectroscopy (IRAS), and scanning tunneling microscopy (STM). Although CV is a most efficient and direct way to obtain important electrochemical parameters, such as the potential range of CO adsorption, the CO oxidation potential, the CO coverage, and the electric capacity of the electrode/electrolyte interface,[2,3] it cannot provide detailed information on adsorbate bonding and adlayer structure on a molecular level. This information is accessible by vibrational spectroscopy and STM, as has been demonstrated by the work of Ito's and Weaver's groups.[4−8]

Although most vibration studies in the past were performed by IRAS, sum-frequency generation (SFG) is a similarly powerful in situ spectroscopy yielding equivalent and/or additional information on surface vibrations.[9] For experiments on massive metal electrodes, both techniques require a thin-layer electrolyte configuration to minimize absorption of the exciting infrared radiation by the electrolyte. This article will elucidate electrochemical implications of thin-layer configurations in spectroelectrochemistry. Although the focus will be on SFG, most of the results apply to conventional infrared spectroscopy as well.

Specifically, we will discuss SFG spectra of CO stretching vibrations on Pt(111) and Pt(110) electrode surfaces in aqueous electrolytes containing 0.1 M $HClO_4$. Consistent with previous infrared absorption studies, we observe a change of site occupation on Pt(111) from 3-fold hollow site/terminal site to bridge site/terminal site when the potential is increased to values positive of the hydrogen adsorption region of the CO-free surface. Our measured frequencies of the internal CO stretching mode on Pt(111) and Pt(110) are in good agreement with previous IRAS work. However, the potentials at which the CO signals disappear in the SFG spectra are considerably lower than the main oxidation potentials in CV.

The disappearance of the CO stretching signals at a comparable potential well below the main oxidation potential of CO was reported recently in an SFG study of CO adsorption on Pt(111) in 0.5 M H_2SO_4 and was interpreted as a transformation of adsorbed CO into a state invisible to SFG; an adsorption geometry with the C−O bond axis nearly parallel to the surface was suggested.[9] Combining SFG spectroscopy and single-frequency SFG measurements, we show that in our experiments CO depletion of the thin-layer electrolyte, caused by oxidation of CO in the layer at potentials below the main oxidation potential in combination with a limited diffusion of CO from the CO-saturated bulk electrolyte, is responsible for the apparent decrease of the oxidation potentials. Our results give no

* Corresponding author. E-mail: w.daum@fz-juelich.de.
† Forschungszentrum Jülich.
‡ Technische Universität München.
§ Present address: Bauer & Partner, D-41468 Neuss, Germany.

10.1021/jp0009148 CCC: $19.00
Published on Web 06/27/2000

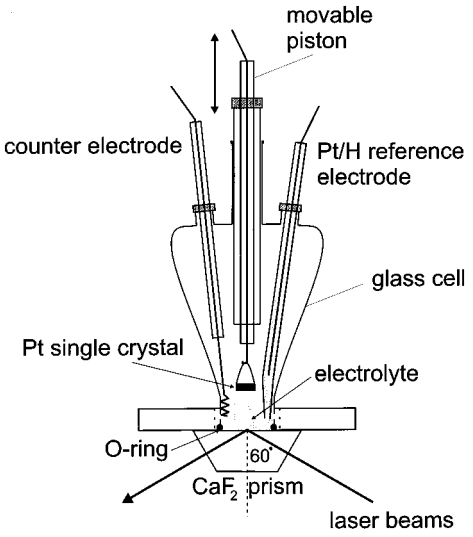

Figure 1. Spectroelectrochemical cell used for cyclic voltammetry and SFG experiments. Inlets for Ar and CO are not shown for the sake of clarity.

indication of an unusual SFG-invisible adsorption state of CO on Pt(111) in perchloric acid solution. The different potential dependencies of SFG and IRAS spectra are related to the different periods of data acquisition. In general, IRAS is much faster than SFG. The effect of CO depletion of the thin-layer electrolyte is therefore much more pronounced in SFG.

II. Experimental Section and Data Analysis

We used cylindrical, (111)- and (110)-oriented Pt single crystals of 10-mm diameter and about 3-mm thickness. The mechanically polished surfaces were oriented to within 0.5° from the nominal surface orientation and were cleaned by prolonged heating in an oxygen atmosphere at 990 °C to deplete the bulk of carbon and sulfur contamination. The crystal surfaces were cleaned using standard flame annealing to red heat in a flame from a propane/butane gas mixture, followed by immediate transfer into the electrochemical glass cell. In the cell, the annealed crystals were allowed to cool for 4 to 6 min in an Ar atmosphere above the aqueous electrolyte to a temperature of less than 100 °C before immersion. Aqueous electrolytes were prepared from purified water (TOC < 10 ppb, specific resistance > 18 MΩ·cm) provided by a Milli-Q Plus system (Millipore, Inc.) and $HClO_4$ (Merck, Suprapur). Cyclic voltammetry and SFG experiments were performed in the electrochemical glass cell shown in Figure 1. As reference electrode, we used a reversible hydrogen electrode (RHE). The reference electrode was charged prior to each experiment by producing a trapped bubble of H_2 gas over a Pt wire in contact with the base electrolyte. All potentials in this work are quoted against this electrode. A Pt wire formed as a coil to increase the area was used as a counter electrode. The electrolyte and the gas volume above it were purged with Ar gas (Messer Griesheim, purity >99.999%), which was introduced to the electrolyte by a gas inlet. For CO adsorption, we used CO gas (Messer Griesheim, purity >99.997%), which was bubbled through the electrolyte by a separate gas inlet. Both gas inlets (not shown in Figure 1) were glass tubes and were similar to the tube containing the reference electrode except for a larger aperture of their tapered ends.

For flame annealing as well as for the experiments in the electrochemical cell, the Pt crystals were suspended on a thick Pt wire with a hook-shaped end. This holding wire was mounted

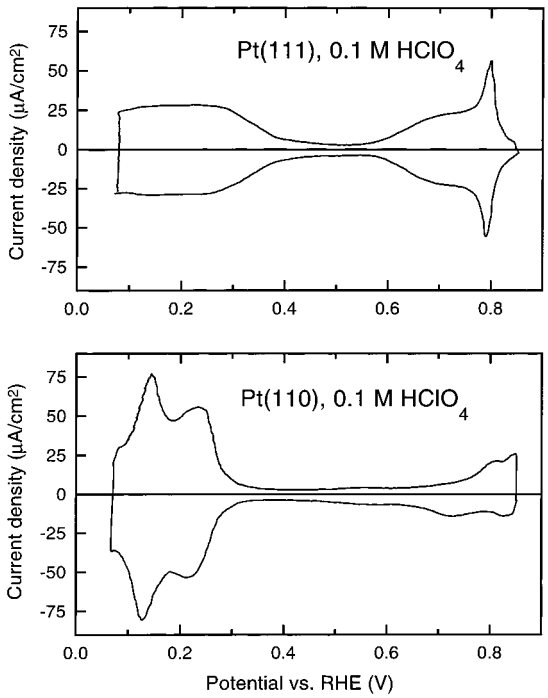

Figure 2. Typical cyclic voltammograms (50 mV s^{-1}) of Pt(111) and Pt(110) surfaces in 0.1 M $HClO_4$.

to a leak-tight, movable glass piston. In this way, the crystals could be lowered to the surface of the electrolyte to make contact with the liquid for cyclic voltammetry, or they could be further immersed into the electrolyte and set down onto the bottom of the cell to make contact with the CaF_2 prism, which served as a laser window for SFG spectroscopy. In the latter case, a thin layer of electrolyte was formed between the electrode surface and the laser window. As discussed below, the effective thickness of this layer was found to be about 2 μm across the laser beams. After flame annealing and cooling the crystal, we recorded voltammograms to ensure the cleanliness and the single-crystal character of the electrode surfaces. Figure 2 shows typical voltammograms of clean Pt(111) and Pt(110) surfaces, respectively, in 0.1 M $HClO_4$. For CO adsorption, we proceeded as follows. After voltammetry of the clean surface in a CO-free electrolyte, the crystal was completely immersed in the electrolyte with the surface not yet brought into contact with the prism. With the electrode potential held at 0.02 V, CO was adsorbed by bubbling the gas for several minutes into the electrolyte until the solution was saturated with CO. To maintain the CO concentration in the bulk solution, this procedure was repeated from time to time during the SFG experiments. All SFG experiments discussed in this work were performed with a CO-saturated electrolyte.

Vibrational spectra of adsorbed CO molecules were obtained by infrared−visible SFG. The vibrations were excited by 19-ps medium infrared pulses from a tunable optical parametric infrared converter operating at a 10-Hz frequency[10] and frequency-upconverted with 22-ps laser pulses of 532-nm wavelength in a near-collinear geometry. Both beams were *p*-polarized, and the angle of incidence was approximately 60°. Only the *p*-polarized component of the sum-frequency signal was detected. Pulse energies were typically 100 μJ for the infrared beam and 400 μJ for the green laser beam. The fluences of both beams were kept below 5 mJ cm^{-2} to reduce laser-induced heating of the samples. To account for the wavelength dependence of the pulse energy and the spatial beam characteristics as well as for laser power drifts and pulse energy

fluctuations, the SFG signal from the sample was normalized to the SFG signal simultaneously generated in the bulk of a polycrystalline ZnS reference sample. Averaging the SFG signal for each infrared frequency over 300 laser pulses, acquisition of a single spectrum from 1700 to 2150 cm^{-1} took about 65 min.

The SFG signal from the Pt/electrolyte interface can be expressed in the form

$$I_{sfg}(\omega_{ir}) = \left|\left(A_0 + \sum_{k=1}^{n} \frac{A_k e^{i\varphi_k}}{\omega_{ir} - \omega_k + i\,\gamma_k/2}\right) F_{zz}^{ir}(\omega_{ir}, d, \theta)\right|^2 \quad (1)$$

In eq 1, the frequency dependence of the sum-frequency susceptibility $\chi^{(2)}$ is assumed as

$$\chi^{(2)} = A_0 + \sum_{k=1}^{n} \frac{A_k e^{i\varphi_k}}{\omega_{ir} - \omega_k + i\,\gamma_k/2} = \chi_{NR}^{(2)} + \chi_R^{(2)}(\omega_{ir}) \quad (2)$$

$\chi^{(2)}$ consists of n vibrational resonances of the adsorbed molecules comprised in $\chi_R^{(2)}(\omega_{ir})$ and a vibrationally nonresonant contribution $\chi_{NR}^{(2)}$.[11] The latter originates from electronic excitations of the substrate that are resonant with the sum frequency[12] and has a spectral dependence that can be neglected on the frequency scale of the molecular vibrations discussed below. The amplitudes A_0, A_k, the vibrational frequencies ω_k, the line widths γ_k (fwhm), and the phases ϕ_k are fit parameters in eq 1. It should be noted that the amplitudes A_k, which characterize the strengths of the vibrational bands in SFG spectra, depend not only on the dynamic dipole moment of the vibration but also on the Raman polarizability of the vibration. $\chi^{(2)}$ includes the contributions of all relevant tensor elements of the surface. These are $\chi_{xxz}^{(2)}$ and $\chi_{zzz}^{(2)}$ if the two laser beams and the sum-frequency beam are *p*-polarized, as is the case in this study.[13]

The function $F_{zz}^{ir}(\omega_{ir}, d, \theta)$ in eq 1, also referred to as the Fresnel factor of the infrared field, quantifies the local electric field strength of the infrared radiation at the position of the adsorbate. It depends on the infrared frequency ω_{ir}, the thickness d of the electrolyte, and the angle of incidence θ of the infrared laser beam. Since the molecules are adsorbed on a metal surface, only the electric field component of the infrared radiation perpendicular to the surface (*z*-direction) can efficiently excite vibrations (dipole selection rule). It is necessary to include this function in the analysis of the spectra because infrared absorption in the electrolyte layer and multiple reflections cause spectral features that are not related to the vibration spectrum of the electrode surface but that modulate the SFG spectrum. The function $|F_{zz}^{ir}(\omega_{ir}, d, \theta)|^2$ was calculated from the dielectric functions of water, Pt, and CaF_2[14] and will be discussed in detail in a forthcoming paper.[12] From fits of eq 1 to the spectra, to be discussed below, we found $d \approx 2\ \mu m$.

III. Results and Discussion

A. CO on Pt(111). Figure 3 displays SFG spectra selected from a series that was obtained after CO adsorption on Pt(111) at 0.02 V. Starting with the adsorption potential, the spectra were recorded for successively more anodic potentials. After each change of potential, the electrode was lifted off the CaF_2 prism to bring the electrode surface in contact with the CO-saturated bulk electrolyte. This way, we ensured that each SFG spectrum was recorded under the condition of an initially CO-saturated thin-layer electrolyte.

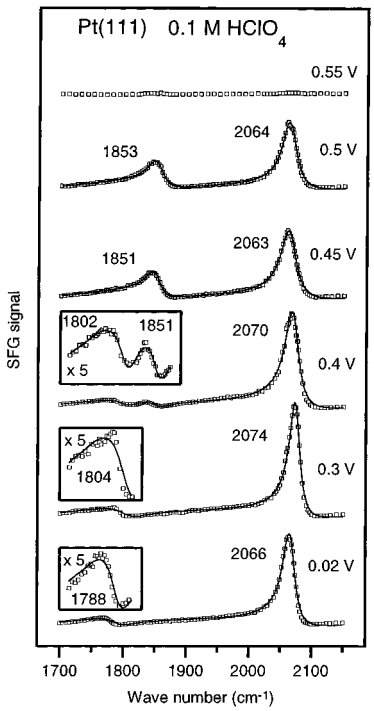

Figure 3. SFG spectra from Pt(111) in 0.1 M $HClO_4$ after adsorption of CO at 0.02 V. Solid lines are fits according to eq 1. The resonance frequencies of the CO stretching modes as obtained from the fits are indicated. The insets display the weak spectral features on a magnified scale. Potentials are versus an RHE.

At 0.02 V, a strong band at 2066 cm^{-1} and a weak band at 1788 cm^{-1} indicate CO adsorption on terminal and 3-fold hollow sites, respectively. This assignment is based on comparison with adsorption experiments on Pt(111) in ultrahigh vacuum[15,16] and on cluster calculations.[17,18] Increasing the potential to 0.3 V results in a blue shift of both bands. The appearance of a third CO stretching mode at 0.38 V with a frequency of 1851 cm^{-1}, which is well resolved in Figure 3 at 0.4 V, signals occupation of additional sites. This frequency agrees with that of CO molecules adsorbed on bridge sites in the c(4 × 2) structure of CO on Pt(111) prepared in ultrahigh vacuum.[15] Increasing the potential to 0.45 V, this mode gains intensity, whereas the signal from CO on 3-fold hollow sites completely disappears. Concomitantly, the frequency of terminal CO is red-shifted. For potentials above 0.5 V, we found the intensities of the two bands to decrease within the acquisition time of the spectrum. At 0.55 V, the CO bands have almost completely disappeared, indicating an almost complete desorption of CO from the Pt(111) surface. It should be noted that the asymmetric line shapes of the bands, most pronounced for the CO mode around 1790 cm^{-1}, results from the addition of a symmetric vibrational line shape to a nonresonant contribution, as described by eq 2.

With regard to the spectroscopic signature of three differently adsorbed CO species on Pt(111) (terminal, bridge, hollow), and with regard to the pairwise occurrence of these species (terminal/hollow at more cathodic potentials, terminal/bridge at more anodic potentials), our SFG spectra are consistent with a number of previous infrared studies. Kitamura et al. observed bands at 1780 and 2068 cm^{-1} at cathodic potentials and bands around 1840−1850 cm^{-1} and 2070 cm^{-1} at more anodic potentials on Pt(111) in 0.5 M H_2SO_4 solutions.[4,5] Comparable results were found by Chang and Weaver in a CO-saturated, 0.1 M $HClO_4$ electrolyte.[6] Later, it was shown that CO adsorption on Pt(111) is largely independent of the solvent and that the occupation of the various sites at saturation coverage is for all solvents

controlled by the applied potential in a uniform way on the scale of a common reference electrode.[19] With respect to the potential dependence $\tilde{\nu}(\phi)$ of the CO stretching frequencies, often referred to as "electrochemical Stark tuning", our spectra yield slopes $d\tilde{\nu}/d\phi$ of about 29, 40, and 57 cm^{-1}/V for terminal, bridge, and hollow sites, respectively, which agree well with results from infrared spectroscopy.[19] For a discussion of the potential dependence of the CO bands, we refer to previous work.[20]

Although vibrational spectroscopy is a suitable technique to provide information on the local adsorption geometry of adsorbed molecules—for CO on Pt it is commonly accepted that the stretching frequency of the molecule is a characteristic signature for a particular adsorption site[17,18]—additional information about the CO overlayer requires structural investigations. In situ STM studies revealed the existence of ordered, compressed CO structures on Pt(111). In a CO-saturated, 0.1 M $HClO_4$ electrolyte, Villegas and Weaver observed a $(2 \times 2)-3CO$ superstructure with a CO coverage of 0.75.[8] For potentials between 0.31 and 0.56 V, they found a $(\sqrt{19} \times \sqrt{19})$ R23.4°−13CO structure with a coverage of 13/19 ≈ 0.68.[8] These two CO structures were also observed by Yoshimi et al.[21] in 0.1 M H_2SO_4. Villegas and Weaver proposed a model for the $(2 \times 2)-3CO$ structure with two molecules per unit cell placed on hollow sites and one molecule placed on top. To reconcile IRAS and STM results for the $(\sqrt{19} \times \sqrt{19})$-R23.4°−13CO structure, they proposed a model with CO molecules in a hexagonal arrangement distributed over on-top, near-on-top, and near-bridge sites.[8] We therefore conclude that our SFG spectra at 0.02 and 0.3 V in Figure 3 correspond to the $(2 \times 2)-3CO$ structure, whereas the appearance of the 1851 cm^{-1} band at 0.38 V is indicative of the $(\sqrt{19} \times \sqrt{19})$R23.4°−13CO structure. We note that the onset of the transition at about 0.38 V, as indicated by our SFG spectra, is in agreement with the STM study by Villegas and Weaver,[8] whereas in IRAS studies the appearance of bridge-bonded CO was observed at about 0.2 V higher potentials.[6,22]

The spectra in Figure 3 show that SFG can be efficiently used to study CO vibrations at Pt/electrolyte interfaces and that SFG yields results that are largely equivalent to IRAS. Nevertheless, a closer inspection of Figure 3 also reveals significant differences such as the very small intensity of the hollow-site vibrations in Figure 3 in comparison with the vibrations on the terminal sites. This seems to contradict the 2:1 occupation ratio of hollow sites versus terminal sites expected for the $(2 \times 2)-3CO$ structure. A lower hollow/terminal intensity ratio than anticipated was also observed in IRAS but to a lesser extent and was explained by dipole−dipole coupling transferring intensity from the hollow-site vibration to the terminal-site vibration.[8]

The much smaller intensity ratio in our SFG spectra (as compared to IRAS) must result from an additional effect that is based on interference in nonlinear optical spectra and that was discussed in detail by Baldelli et al. in a recent SFG study of CO adsorption on Pt(111) in sulfuric acid electrolytes.[9] These authors measured SFG spectra of CO stretching vibrations with different polarizations of the fundamental and sum-frequency beams. With the two laser beams and the SFG beam *p*-polarized (*ppp*), their spectra displayed only the band for terminal CO while appreciable intensity from CO on hollow sites was observed for *s*-polarization of the visible laser beam and of the sum-frequency signal (*ssp*). They showed that the absence of CO vibrations on hollow sites in their *ppp*-spectra results from destructive interference of the two sum-frequency susceptibility tensor elements $\chi^{(2)}_{xxz}$ and $\chi^{(2)}_{zzz}$. For terminal CO, the interference

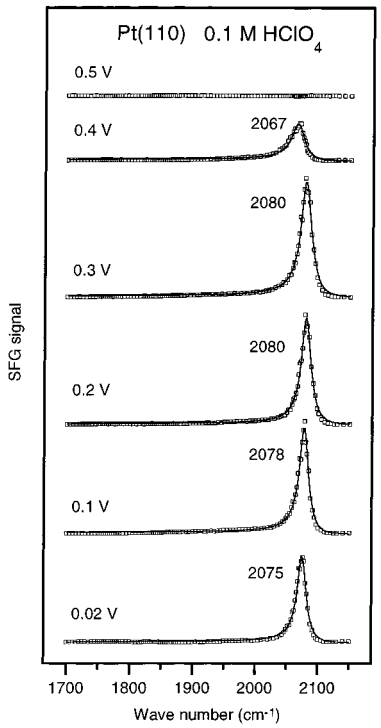

Figure 4. SFG spectra from Pt(110) in 0.1 M $HClO_4$ after adsorption of CO at 0.02 V. Solid lines are fits according to eq 1. The resonance frequencies of the CO stretching mode as obtained from the fits are indicated. Potentials are versus an RHE.

is not destructive because of smaller in-plane elements of the Raman polarizability tensor, leading to a smaller contribution of $\chi^{(2)}_{xxz}$ relative to $\chi^{(2)}_{zzz}$.[9] Our SFG spectra in Figure 3 do exhibit discernible, albeit weak, intensity from CO on hollow sites, suggesting incomplete destructive interference of $\chi^{(2)}_{xxz}$ and $\chi^{(2)}_{zzz}$. This difference between our spectra and those by Baldelli et al. can be explained by different angles of incidence of the two laser beams in our experiments, leading to different interference conditions.

B. CO on Pt(110). SFG spectra after CO adsorption on Pt(110) are shown in Figure 4. They exhibit a single band characteristic of terminal CO adsorption with the frequency increasing from 2075 cm^{-1} to 2080 cm^{-1} between 0.02 and 0.3 V. A decrease of frequency and intensity of this band, starting at ∼0.38 V and advanced at 0.4 V, indicates partial desorption at these potentials, as the coverage dependence of frequency and intensity of this CO band is well documented.[24] Above 0.45 V, CO is completely desorbed from Pt(110). The exclusive occupation of terminal sites on Pt(110) is in agreement with previous spectroscopic work performed in ultrahigh vacuum[16,23] and at the Pt(110)/electrolyte interface.[6,24,25] The CO frequency and its potential dependence ($d\tilde{\nu}/d\phi \approx 28$ cm^{-1} between 0.02 and 0.2 V) are in good agreement with IRAS results by Chang and Weaver[6,24] for saturation coverage. We point out that we use the notion "terminal adsorption" for CO on Pt(110) in a rather loose way that also includes a possible bonding configuration, which deviates from a strictly perpendicular configuration. For the (2×1)p2mg structure formed at high CO coverages at the Pt(110)/vacuum interface, it was shown that the molecular axes of the adsorbed CO molecules are tilted away from the surface normal.[26] Since spectroscopy of the C−O stretching mode alone does not allow us to distinguish between terminal adsorption and near-terminal adsorption with a tilted molecular axis—frequencies and intensities are largely determined by the coverage-dependent dipole−

dipole interaction[16,23]—the latter adsorption configuration is also conceivable for high coverages of CO at the Pt(110)/electrolyte interface.

C. Effects of Thin-Layer Electrolytes. A noticeable result of the present study is that the CO bands disappear in our spectra at potentials well below the potential at which the main CO oxidation current peak is observed in CV. For CO on Pt(111), we find that the SFG vibration bands of CO on both bridge and terminal sites (Figure 3) disappear at 0.55 V on the time scale of several minutes, well within the acquisition time of the spectrum, whereas the main oxidation in a CO-free electrolyte occurs at about 0.78 V.[3] For Pt(110) the vibration band of adsorbed CO disappears in our SFG spectra at about 0.45 V (Figure 4), again well below the main oxidation potential at about 0.68 V for CO on Pt(110) in a CO-free 0.1 M $HClO_4$ electrolyte.[3]

The disappearance of the CO bands in our SFG experiments with Pt(111) for $\phi > 0.5$ V (Figure 3) can be explained in a consistent way if we take into account that in CO-saturated electrolytes of 0.1 M $HClO_4$, a weak but measurable oxidation occurs at considerably lower potentials than 0.78 V. In CV, this oxidation is observed as a "preoxidation wave" starting at about 0.5 V, whereas the main oxidation of CO proceeds only for potentials above 0.85 V in a CO-saturated electrolyte.[22] Spectroscopic evidence for CO oxidation in the potential range of the preoxidation wave was gained by IRAS experiments in which the presence of CO_2 in the electrolyte was observed as a weak absorption band at 2345 cm^{-1} for potentials as low as 0.5 V.[22]

Although in a CO-saturated bulk electrolyte the desorption of electro-oxidized CO from the surface is compensated by continuous readsorption from the electrolyte, resulting in a constant CO coverage for potentials within the preoxidation wave, the situation can be much different for a very thin electrolyte, as was used in the present SFG experiments. It is well known that in an electrolyte with a thickness of only a few microns the concentration of electrolyte species taking part in reactions at the electrode surface depends on the diffusion of these species from the bulk electrolyte into the layer.[27] For a sufficiently large reaction rate, the thin electrolyte layer between the CaF_2 prism and the Pt surface can therefore be considered as largely isolated from the surrounding bulk electrolyte. With limited diffusion of CO into the thin layer, CO oxidation could eventually lead to CO depletion of the thin-layer electrolyte, with a volume of less than 4×10^{-4} mL in our experiments, and, as a consequence, to a continuous decrease of adsorbed CO within the acquisition time of an SFG spectrum.

We were able to prove this hypothesis by potential variation in a single-frequency SFG experiment. These measurements could be performed on a much faster time scale (30 s) than the spectra in Figure 3 and were therefore not subjected as much to the diffusion limitations of the thin-layer configuration. However, it was not practicable to use the frequency of a CO vibration line to monitor the presence of adsorbed CO because the potential dependencies of the CO frequencies as shown in Figure 3 cause a strong potential dependence of the SFG intensity in a single-frequency experiment even if the CO coverage does not change.

Instead, we employed a different tactic, using SFG at a frequency for which the SFG intensity is strongly correlated with CO adsorption, that is, at which the intensity closely follows the potential dependence of CO adsorption and desorption but the frequency dependence is nearly independent of the potential. This tactic becomes more transparent by inspection of Figure 5, which displays SFG spectra after CO adsorption on Pt(111) that is measured in a wider frequency range, from 1800 to 3300 cm^{-1} for potentials between 0.02 and 0.6 V. Similar to Figure 3, it shows the band of CO on terminal sites, and at 0.5 V, the band of CO on bridge sites. In addition, Figure 5 exhibits a strong and spectrally broad resonant signal between 2400 and 3000 cm^{-1} with a spectral dependence that does not change between 0.02 and 0.5 V. Furthermore, the SFG intensity in this range is almost independent of the potential up to 0.5 V and disappears together with the CO bands for potentials above 0.5 V. The nature of these excitations will be discussed in detail in a forthcoming publication. As we shall show elsewhere,[12] the SFG signal in this spectral range originates from electronic transitions in the Pt surface that are resonant with the sum-frequency and from O−H stretching vibrations in the double layer with frequencies considerably red-shifted from those of bulk water molecules (~3400 cm^{-1}) and inhomogeneously distributed over a wide spectral range. The SFG signal from both contributions depends on the surface charge in a characteristic way, such that a more negatively charged surface will lead to a larger resonant SFG signal between 2400 cm^{-1} and 3000 cm^{-1}.[12] It should be noted that the decrease of SFG intensity above 2900 cm^{-1} in Figure 5 originates from infrared laser power absorption by bulk water stretching vibrations in the thin-layer electrolyte. We point out that a resonant SFG signal between 2400 cm^{-1} and 3000 cm^{-1} is not unique to a CO-covered Pt electrode. This signal is also observed for clean Pt surfaces in aqueous acidic electrolytes but with a very different potential dependence of its intensity: for a clean Pt(111) electrode surface, the intensity continuously decreases from a maximum at 0 V to almost zero at the onset of OH adsorption (~0.6 V),[12] whereas for a CO-covered electrode, it is essentially constant up to the potential at which the CO adlayer is desorbed (Figures 5 and 6). The SFG signal between 2400 and 3000 cm^{-1} can therefore be used to monitor desorption of electro-oxidized CO from an initially CO-covered Pt(111) surface.

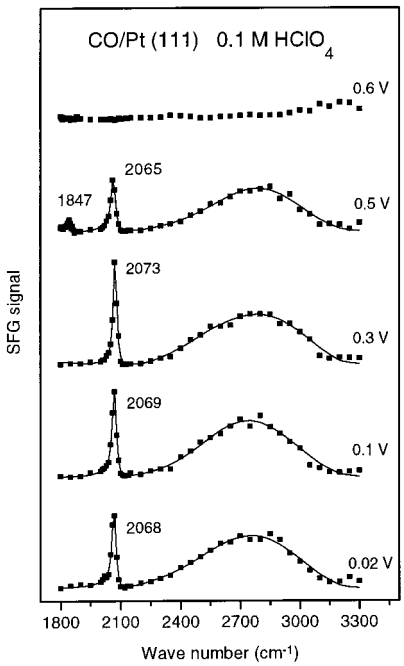

Figure 5. SFG spectra from Pt(111) in 0.1 M $HClO_4$ after adsorption of CO at 0.02 V. Lines are guides to the eyes. Data sampling: 200 pulses per frequency. Potentials are versus an RHE.

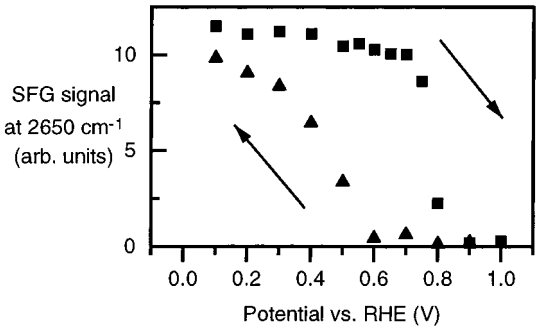

Figure 6. Squares represent an anodic sweep of the SFG signal at 2650 cm^{-1} from a CO-covered Pt(111) surface in an initially CO-saturated thin-layer electrolyte, followed by a cathodic sweep (triangles) after electro-oxidation. Adsorption potential: 0.02 V.

Figure 6 shows the result of a potential variation when the sum-frequency was generated using an infrared frequency of 2650 cm^{-1}. With an initially CO-saturated thin-layer electrolyte and a saturated layer of CO adsorbed at 0.02 V, the potential was successively increased and the SFG intensity monitored without lifting the electrode off the prism. Each data point represents an average of the SFG signals of 300 laser pulses (30 s). A pause of 3 s between two consecutive measurements was used to change the potential. As expected from the data in Figure 5, the SFG intensity changes little between 0.1 and 0.5 V, except for a small drop in intensity between 0.4 and 0.5 V that may be attributed to the structural transition in the CO adlayer. In contrast to Figure 5, however, the SFG signal remains nearly constant between 0.5 and 0.7 V, and the presence of only a moderate decrease of SFG intensity at 0.75 V indicates substantial CO adsorption, even at this potential. This is in marked contrast to a clean Pt(111) electrode, which does not generate a significant sum-frequency signal at 2650 cm^{-1} for potentials above 0.5 V.[12] The SFG signal vanishes between 0.8 and 0.85 V, indicating complete desorption of CO in this potential range. At 1.0 V, the direction of the potential scan was reversed without lifting the electrode off the prism. In contrast to the behavior on the anodic sweep, a significant SFG signal was detected only for potentials at and below 0.5 V, and the original signal strength was recovered only for potentials close to that of the hydrogen evolution reaction. The potential dependence of the SFG signal in the cathodic sweep corresponds to that of a clean Pt(111) electrode in 0.1 M $HClO_4$ with comparatively little SFG intensity at 0.5 V, as shown and discussed elsewhere.[12]

After completing the cathodic scan in Figure 6, we checked whether CO was adsorbed at the final potential of 0.1 V by monitoring the SFG signal from terminally adsorbed CO at 2070 cm^{-1} and found only about 1/8 of the signal from a saturated CO layer. This signal level agrees with that of a clean Pt(111) surface at 0.1 V and can be accounted for by electronic excitations of the surface[12] with little, if any, contribution from the stretching vibrations of adsorbed CO. Upon shortly lifting the electrode off the prism, the signal at 2070 cm^{-1} was restored to the original level of a saturated $(2 \times 2)-3CO$ adlayer. This result unambiguously proves that after the oxidation cycle, the thin-layer electrolyte was largely depleted of CO although the surrounding bulk electrolyte was saturated with CO.

We also have cross-checked the simultaneous appearance of SFG signals from the stretching band of terminally adsorbed CO and from the transitions at 2650 cm^{-1} for potentials above 0.5 V, that is, in the potential range of the preoxidation wave. In contrast to the measurement shown in Figure 6, after changing the potential (in steps of 0.1 V between 0.1 and 0.5 V and in steps of 0.05 V above 0.5 V) a time of 120 s was allowed to pass before continuing with the next SFG measurement (300 laser pulses). After the measurement at 0.65 V (with a strong signal at 2650 cm^{-1}) and an increase of the potential to 0.7 V, we checked the SFG signal at 2070 cm^{-1} during the holding time and found a strong intensity, comparable to that at 0.1 V. Repeating the same procedure after the measurement at 0.7 V, the signal at 2650 cm^{-1} had dropped by one order of magnitude to nearly zero, and the signal from terminal CO had dropped by a factor 4. After the measurement at 0.75 V, no significant signal was observed at either frequency. These experiments also provide information on the time scales of CO desorption in our thin-layer electrolytes: at 0.65 V, it takes more than 150 s, and at 0.7 V less than 150 s, for significant desorption to occur. These time scales are consistent with those observed in a recent IRAS study by Akemann et al.[22]

Combining the results from Figures 5 and 6, we can draw the following conclusions: (a) For an initially CO-saturated thin-layer electrolyte, CO remains adsorbed on Pt(111) even at potentials as high as 0.75 V on a time scale of several seconds (anodic sweep in Figure 6). (b) After complete oxidation of all CO molecules on the surface, significant readsorption of CO does not occur (on a time scale of several minutes) when the potential is decreased to values within the double-layer region or even within the hydrogen adsorption region of the clean Pt(111) surface (cathodic sweep in Figure 6). The volume of the thin-layer electrolyte must therefore be depleted of CO, proving that restoration of a sufficiently large CO concentration by diffusion from the surrounding CO-saturated bulk electrolyte is largely suppressed. (c) With this diffusion limitation and a sufficiently large oxidation rate above 0.5 V, the dynamic equilibrium between CO desorption due to oxidation and readsorption from the electrolyte, which is necessary for a constant CO coverage, cannot be maintained above a certain potential in the range of the preoxidation wave. Our spectra in Figures 3 and 5 show that the diffusion limitation is not yet effective at 0.5 V, whereas at 0.55 V it clearly is.

This scenario of CO oxidation in a thin-layer electrolyte is consistent with all experimental results presented above and explains why, in our SFG spectra, CO desorption from Pt(111) is already observed at potentials above 0.5 V although the main oxidation of CO in large electrolyte volumes does not occur below 0.75 V.

Whereas this kinetic effect of the thin-layer configuration becomes quite apparent in our SFG study, the conclusions also apply to IRAS. However, since the oxidation effects discussed above depend on the time scale of the experiment, and since Fourier transform IRAS experiments are usually performed much more quickly than conventional SFG experiments,[28] one expects this effect to be far less pronounced in IRAS. In fact, the bands of terminal and bridge-bonded CO on Pt(111) in a CO-saturated $HClO_4$ electrolyte were observed in IRAS for potentials as high as 0.7 V.[6,22]

Interestingly, the CO bands observed by Baldelli et al. in their SFG study of CO adsorption on Pt(111) in a 0.5 M H_2SO_4 electrolyte also disappeared at a potential of about 0.55 V (vs Pd/H).[9] However, from CO stripping experiments they found that most of the CO was still adsorbed on the surface, even after holding the potential for 15 minutes at 0.6 V. Therefore, they concluded that at ~0.55 V, the CO molecules are transformed into a state that is invisible to SFG, and they suggested an adsorption configuration with the CO bond axis nearly parallel to the surface.[9] This is a remarkable result because such an adsorption state is very unusual for CO and

was not observed in previous studies of CO on Pt(111) with various electrolytes.[19]

Our discussion above shows that the spectroscopic results of our study are consistent with CV if the specific effects of the thin-layer electrolyte are considered. We do observe adsorbed CO in our SFG experiments for potentials of the preoxidation wave, and we do not find indications for an adsorption state that is invisible to SFG, as proposed by Baldelli et al. Also, a nearly flat adsorption of CO would lead to a substantial decrease of infrared absorption of the CO stretching vibrations, which was not observed in previous IRAS experiments, even at 0.7 V.[6,22] Given the fact that a $(2 \times 2)-3CO$ structure with comparable CO stretching frequencies[9] is formed on Pt(111) in both $HClO_4$[8] and H_2SO_4[29] electrolytes, and considering the fact that the stronger anion adsorption for H_2SO_4 is effectively suppressed when CO is adsorbed, different adsorption geometries of CO on Pt(111) in the two electrolytes for potentials above 0.5 V would be an unexpected result.

We expect the phenomenon of CO desorption from surfaces at potentials well below the main oxidation potential to be a general phenomenon for electrochemical thin-layer systems with sufficiently strong preoxidation. It is very likely that the low potential of ~0.45 V, at which the CO band completely disappears in our SFG spectra of the Pt(110) surface (Figure 4), is also related to preoxidation in combination with hindered exchange of CO with the bulk electrolyte. The situation is more complicated for the Pt(110) surface, however, since this surface is known to reconstruct into a (1×2) structure or to remain unreconstructed, depending on the preparation conditions.[30] We have reason to believe that our preparation procedure described in section II yields a reconstructed Pt(110) electrode surface: after application of this procedure to the Pt(110) surface and in a 0.5 M electrolyte of H_2SO_4, we observed a voltammogram of the clean surface that corresponds to that published by Marković et al. for the reconstructed Pt(110)(1×2) surface.[30] Since the CO stripping voltammogram of the Pt(110)(1×2) surface in H_2SO_4 exhibits a preoxidation wave starting at about 0.4 V,[30] we believe that preoxidation is also effective in $HClO_4$.

IV. Conclusion

We have shown, by comparing SFG spectra with single-frequency measurements, that preoxidation is an effective mechanism for CO desorption in experiments utilizing a thin-layer electrolyte configuration. The diffusion limitation of this configuration has to be considered when results from different experiments with different time scales are compared. Although this kinetic effect is not restricted to SFG, it appears quite pronounced in our SFG experiments because of the comparatively long periods of spectra acquisition. In consideration of this effect, the disappearance of the CO bands in our SFG spectra at potentials of the preoxidation regime is understandable and consistent with cyclic voltammetry and IRAS. SFG and IRAS are in harmony regarding the observation of different CO adsorption states on Pt(111) and a single state on Pt(110).

References and Notes

(1) Igarashi, H.; Fujino, T.; Watanabe, M. *J. Electroanal. Chem.* **1995**, *391*, 119.
(2) Orts, J. M.; Fernández-Vega, A.; Feliu, J. M.; Aldaz, A.; Clavilier, J. *J. Electroanal. Chem.* **1992**, *327*, 261.
(3) Clavilier, J.; Albalat, R.; Gomez, R.; Orts, J. M.; Feliu, J. M.; Aldaz, A. *J. Electroanal. Chem.* **1992**, *330*, 489.
(4) Kitamura, F.; Takeda, M.; Takahashi, M.; Ito, M. *Chem. Phys. Lett.* **1987**, *142*, 318.
(5) Kitamura, F.; Takahashi, M.; Ito, M. *Surf. Sci.* **1989**, *223*, 493.
(6) Chang, S.-C.; Weaver, M. J. *Surf. Sci.* **1990**, *238*, 142.
(7) Oda, I.; Inukai, J.; Ito, M. *Chem. Phys. Lett.* **1993**, *203*, 99.
(8) Villegas, I.; Weaver, M. J. *J. Chem. Phys.* **1994**, *101*, 1648.
(9) Baldelli, S.; Markovic, N.; Ross, P.; Shen, Y.-R.; Somorjai, G. *J. Phys. Chem. B* **1999**, *103*, 8920.
(10) Krause, H.-J.; Daum, W. *Appl. Phys. B* **1993**, *56*, 8.
(11) Zhu, X. D.; Suhr, H.; Shen, Y. R. *Phys. Rev. B* **1987**, *35*, 3047.
(12) Dederichs, F.; Friedrich, K. A.; Akemann, W.; Daum, W. To be submitted for publication.
(13) The last tensor index refers to the respective coordinate of the infrared field.
(14) *Handbook of Optical Constants of Solids I−III*; Palik, E. D., Ed.; Academic Press: San Diego, 1998.
(15) Schweizer, E.; Persson, B. N. J.; Tüshaus, M.; Hodge, D.; Bradshaw, A. M. *Surf. Sci.* **1989**, *213*, 49.
(16) Klünker, C.; Balden, M.; Lehwald, S.; Daum, W. *Surf. Sci.* **1996**, *360*, 104.
(17) Müller, J. E. *The Chemical Physics of Solid Surfaces*; King, D. A., Woodruff, D. P., Eds.; Elsevier: Amsterdam, 1993; Vol. 6, p 29.
(18) Daum, W.; Dederichs, F.; Müller, J. E. *Phys. Rev. Lett.* **1998**, *80*, 766.
(19) Chang, S.-C.; Jiang, X.; Roth, J. D.; Weaver, M. J. *J. Phys. Chem.* **1991**, *95*, 5378.
(20) Chang, S. C.; Weaver, M. J. *J. Chem. Phys.* **1990**, *92*, 4582.
(21) Yoshimi, K.; Song, M.-B.; Ito, M. *Surf. Sci.* **1996**, *368*, 389.
(22) Akemann, W.; Friedrich, K. A.; Stimming, U. *J. Chem. Phys*., submitted for publication.
(23) Bare, S. R.; Hofman, P.; King, D. A. *Surf. Sci.* **1984**, *144*, 347.
(24) Chang, S.-C.; Weaver, M. J. *Surf. Sci.* **1990**, *230*, 222.
(25) Jiang, X.; Weaver, M. J. *Surf. Sci.* **1992**, *275*, 237.
(26) Rieger, D.; Schnell, R. D.; Steinmann, W. *Surf. Sci.* **1984**, *143*, 157.
(27) Iwasita, T.; Nart, F. C. *Prog. Surf. Sci.* **1997**, *55*, 271.
(28) Most advanced SFG spectrometers exploit the self-dispersive nature of the SFG process and are capable of very fast data acquisition comparable to or even faster than FTIRAS. See, for example, Richter, L. J.; Petralli-Mallow, T. P.; Stephenson, J. C. *Opt. Lett.* **1998**, *23*, 1594.
(29) Marković, N. M.; Grgur, B. N.; Lucas, C. A.; Ross, P. N. *J. Phys. Chem. B* **1999**, *103*, 487.
(30) Marković, N. M.; Grgur, B. N.; Lucas, C. A.; Ross, P. N. *Surf. Sci.* **1997**, *384*, L805.